ACS OMEGA

http://pubs.acs.org/journal/acsodf

Article

Potential Acetylcholinesterase Inhibitor Acting on the Pesticide Resistant and Susceptible Cotton Pests

Seethalakshmi Sakthivel, Habeeb Shaik Mohideen,* Chandrasekar Raman, and Saharuddin Bin Mohamad

Cite This: *ACS Omega* 2022, 7, 20515−20527

Read Online

ACCESS | Metrics & More | Article Recommendations | Supporting Information

ABSTRACT: Gossypium spp., produces economically important cotton fiber, and its yield is highly affected due to pest attacks. Insecticidal target site mutation is one of the reasons behind insecticide resistance to a wide range of pesticides. Acetylcholinesterase (AChE) protein sequences from major pests of cotton were analyzed to assess various physicochemical properties, presence of motifs, and understand evolutionary relationship. The impact of three mutant AChE1, *A. lucorum* A216S, *B. tabaci* F392W, and *A. gossypii* A302S, on the strucutral stability was assessed, and F392W_AChE1 was selected based on 100 ns molecular dynamics simulation. Virtual screening of the zinc database and high-throughput virtual screening, standard precision, and extra precision docking resulted in the identification of six compounds. The six identified compounds and six known commercial pesticdes were docked with three mutant and three wild type AChE1, and one (C1) was selected based on Tice criteria. The conformational and interaction stability of the AChE1-C1 and F392W_AChE1-C1 complexes were monitored at 100 ns Gromacs simulation and were found to be thermodynamically favorable. Therefore, C1 may have the potential to bind to the resistant and susceptible strains of cotton pest, and the resistance developed by insects could be arrested. Furthermore, synthesis and field study of C1 will lead us to a better understanding of the efficacy of the identified compound.

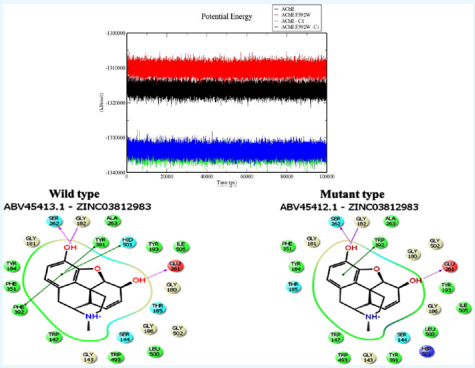

INTRODUCTION

Sustaining food security on par with the ever-growing population is a challenge to agricultural productivity. Modern farming practices have resulted in a better yield from various crops of social and economic importance.[1] However, there are still challenges such as dependence on rainfall, pest attack, and soil erosion, among others.[2]

Cotton fiber producing the Gossypium species holds commercial significance globally. India is the largest producer of cotton (29 million bales, 2019−2020), but its productivity/hectare achieved is not on par with other nations.[3] One of the prominent reasons for the reduced yield of cotton is insect pests and crop diseases. Effective control of insect pests is crucial for better crop yield and also in containing insect-borne conditions.[4] Pesticides such as organophosphates (OP) and organochlorines (OC) are widely used to control insect pests by seed treatments and foliar applications.[5] Prolonged and intensive pesticide application has resulted in pest resurgence and pesticide resistance.[6] Over 500 studies have reported a decrease in the effect of insecticides due to insecticide resistance.[7]

Genetic modifications such as transcriptional changes and point mutations in coding regions render insecticide resistance to insects. These allow higher rates of insecticide detoxification and result in target site insensitivity.[8] Another important mechanism for insecticide resistance is metabolic resistance. Detoxification enzymes in insects can block or hydrolyze the insecticide before it reaches the target site.[9]

Acetylcholinesterases (AChE) are catalytically active enzymes belonging to the multigene carboxylesterase family found across the species.[10] Insecticides such as OP and carbamates usually phosphorylate or carbamylate the serine residue present in the active pocket of AChE to inhibit its activity.[11] This process results in the accumulation of acetylcholine in the synapses, leaving the acetylcholine receptor permanently open, increasing the excitement in nerves, leading to insect death.[12] An altered AChE insensitive to the active metabolite can escape from the adverse effects of insecticides.[13]

Extensive loss of biodiversity and land degradation are due to the usage of synthetic pesticides and herbicides. Implementation of organic farming practices is highly recommended as a part of UN Sustainable Development Goals 2030 (SDG).[14] Therefore,

Received: December 29, 2021
Accepted: May 27, 2022
Published: June 7, 2022

https://doi.org/10.1021/acsomega.1c07359
ACS Omega 2022, 7, 20515−20527

plant-based organic chemical compounds are a better option for biocontrol measures.[15]

Molecular modeling approaches of bioinformatics have enhanced the understanding of biological systems. They have also helped in the identification of alternative compounds[16,17] to inhibit targets such as AChE.[18] Several studies have employed high throughput virtual screening,[19] QSAR,[20,21] molecular docking,[22−24] and molecular dynamics[25] for identifying potential inhibitors to AChE, while other approaches have also been used to study the mutations in this enzyme. Structural instability due to the breaking of intermolecular hydrogen bond has been attributed to variations in AChE1.[26] Mutations in AChE analyzed from different insect pests are found to alter the interaction between OP and AChE, thereby affecting the phosphorylation of the enzyme.[22] Pesticides such as OP are proven to induce toxicity in humans by interfering with their metabolic pathways.[27]

Due to the above reasons, it becomes a necessity to find solutions to address the issue of pesticide resistance. Considering the importance of active site-based mutation, we performed a comparative analysis of AChE coding genes from eight major cotton pests, and preference was given to AChE from insecticide resistance strains. Natural compounds having an inhibitory effect on AChE from insecticide-resistant and insecticide-susceptible strains were identified by virtual screening, molecular docking, and molecular dynamics simulation studies.

MATERIALS AND METHODS

Data Retrieval. A flowchart illustrating the methodology employed in this study is shown in Figure 1. Insect specific (keywords- insect/insecta) 1710 AChE sequences (keywords, "acetylcholinesterase", "acetyl cholinesterase", "acetylcholine esterase", and "ACHE or AChE") were downloaded from the NCBI protein database. Cotton pest-specific sequences were used to perform multiple sequence alignment using the ClustalW module in MEGA7.[28] Redundant sequences (100% identity) were discarded using Elimdup, and 24 (>250 AA) sequences were considered for further study.

Multiple sequence alignment involving 24 unique sequences was used to generate a residue-wise similarity graph using Plotcon (http://www.bioinformatics.nl/cgi-bin/emboss/plotcon). A neighbor-joining method-based phylogenetic tree was constructed with 1000 bootstrap replicates based on the Jones−Taylor−Thornton (JTT) model.

3D Structure Prediction and Model Validation. The experimental structure of any cotton-pest specific AChE was not available. So, 3D models of 24 AChE sequences were generated using the Swiss-model workspace server.[29] Modeled structures were validated using the different programs available at the Structural Analysis and Validation Server (SAVES) and the Ramachandran plot using the RAMPAGE server.[30]

Physicochemical Properties and Mutation Analysis. The physicochemical properties were computed using Protparam,[31] putative protein motifs were identified using Multiple Em for Motif Elicitation (MEME) suite,[32] and amino acid compositions were calculated using our in-house Perl script. Mutations in AChE were identified from the literature, and the impact of point mutation on protein stability was ascertained using I-Mutant Server2.0.[33]

Conformational Stability Using Molecular Dynamics Simulation. Structural flexibility and conformational stability of the highly deleteriously mutated (F392W) and wild type

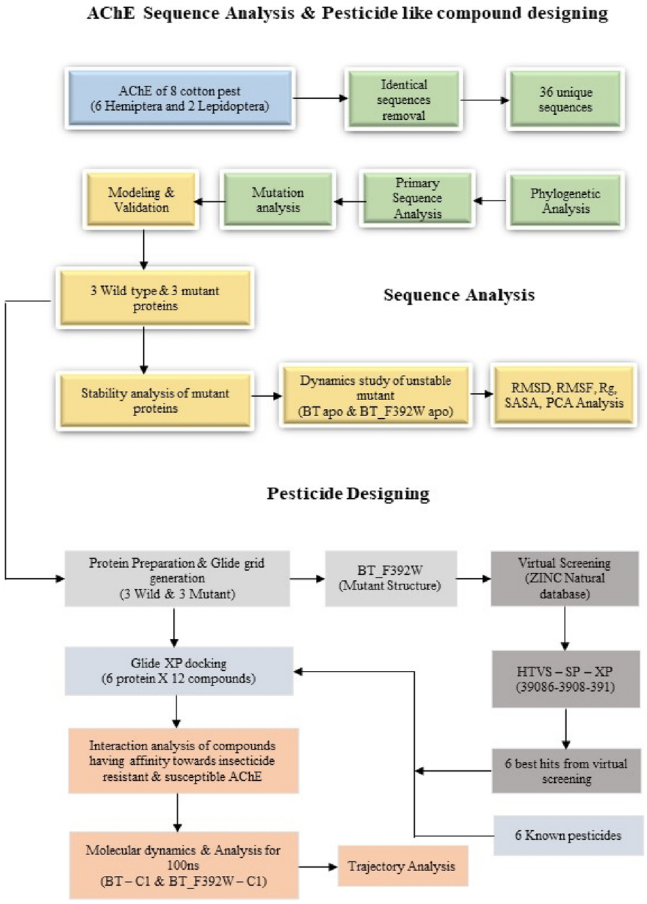

Figure 1. Steps involved in the analysis of AChE mutation and pesticide-like compound designing. Color codes: blue: input dataset; green: first phase involving sequence analysis; yellow: second phase involving analysis of the structural impact of point mutation using molecular modeling studies; light gray: docking preparation; blue-gray: XP docking; dark gray: virtual screening procedure; orange: molecular dynamics and interaction analysis.

structures were studied using molecular dynamics simulation (MDS) for a period of 100 ns using Gromacs version 4.5.3 installed on the High-Performance Computer Cluster (SRM-HPCC). Protein topology parameters were obtained by implementing GROMOS96 force field. Each system was immersed into an SPC water model in a cubical box with a minimal distance of 10 Å from the protein surface to the edge of the box. A periodic boundary condition was applied such that the number of particles, pressure, and temperature remained constant throughout the simulation. Eleven sodium ions were added to neutralize the system. Unfavorable contacts in each system were energy minimized, and the temperature was maintained by applying the Berendsen algorithm.[34] Final production MD was carried out for 100 ns using the isothermal−isobaric (NPT) ensemble. During the simulation, the temperature was maintained constant at 300 K. To treat long-range Coulombic interactions, the particle mesh Ewald method[35] was used. LINCS algorithm[36] was applied to measure bond lengths between hydrogen bonded atoms, and a time step of 2 fs was allowed. Coulombic interactions were truncated at 0.9 nm, and the van der Waals force was maintained constant at 1.4 nm.[37]

Principal Component Analysis. Advanced analysis of trajectories generated from MDS was done using essential

https://doi.org/10.1021/acsomega.1c07359
ACS Omega 2022, 7, 20515−20527

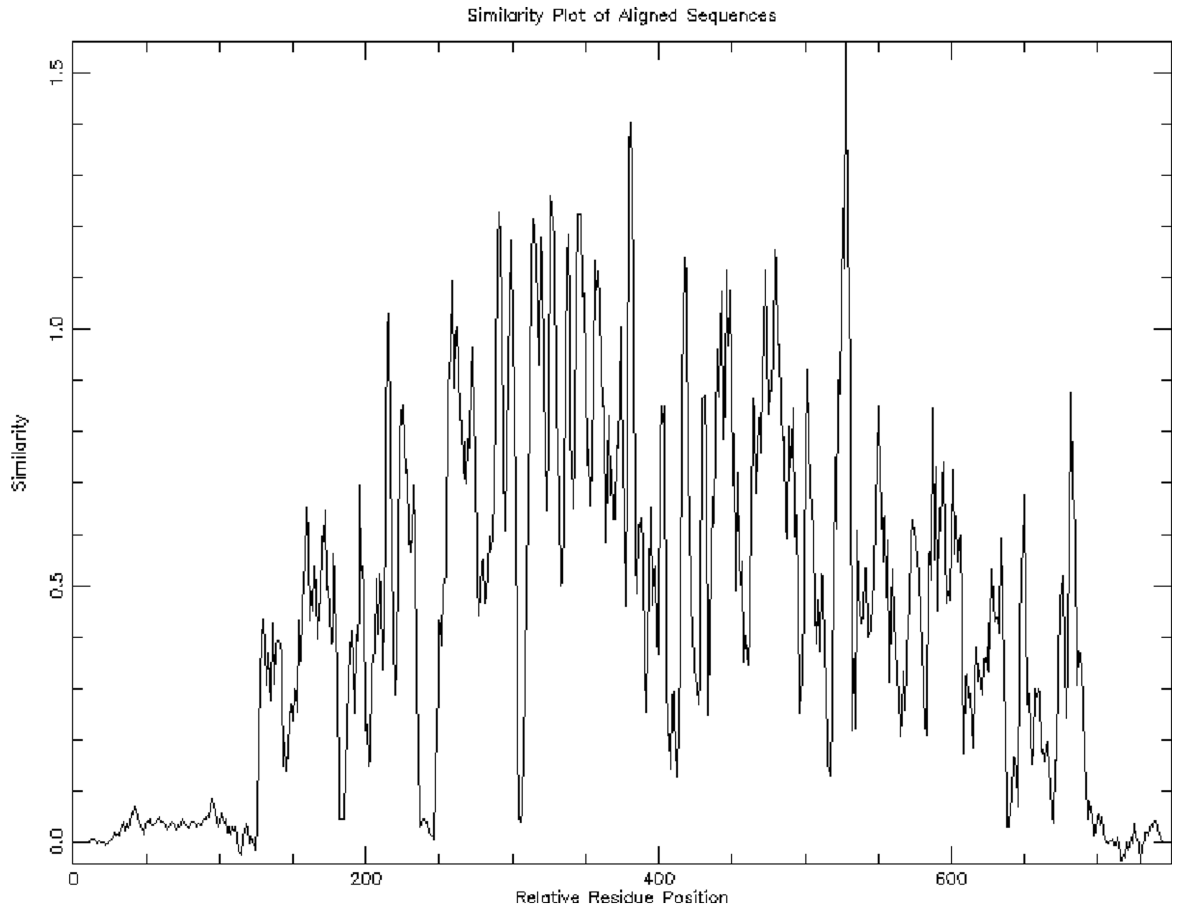

Figure 2. Similarity profile of AChE aligned sequences. The horizontal axis represents the relative residue position and the vertical axis represents the similarity.

dynamics. From principal component analysis (PCA), the motion of the protein was determined by extracting the concerted movement of the protein in different frames during the simulation. PCA was done in two steps: (i) constructing a variance/covariance matrix using C-alpha atoms and (ii) diagonalization of the covariance matrix. PCA was performed using *g_anaeig* and *g_covar* tool of Gromacs.[38]

Ligand and Protein Preparation. Zinc natural database (156,601 compounds)[39] and six known cotton pest pesticides (chlorpyrifos (OP), malathion (OP), acephate (OP), methomyl (C), thiodicarb (C) and deltamethrin (P)) structures were downloaded and prepared using the Ligprep module of Maestro 10.2 (Maestro v 10.2 Schrodinger LLC, New York, NY). During ligand preparation, the pH was set to 7.0, and the tautomeric and ionization states were prepared using the Epic module. A maximum of 32 conformers were generated for each ligand structure.[37] The native and mutant AChE proteins were prepared using the protein preparation wizard of Maestro, and the structures were energy minimized using the Optimized Potentials for Liquid Simulations 2005 (OPLS2005) force field. A cubic grid box (gridbox X, Y, and Z ranges were 30, 30, and 30, respectively) was created around the active site comprising SER262, HIS501, GLU388, and TRP392 of AChE protein.

Virtual Screening. Mutant protein (Genbank acc: ABV45412.1, *Bemisia tabaci* F392W mutation) was used for further study. Virtual screening and Tice rule[40] based filtering was employed to identify compounds that could have the potential to inhibit AChE in both insecticide-resistant and insecticide-susceptible strains. The Glide docking program was used to perform virtual screening in the following order: high-throughput virtual screening (HTVS), standard precision (SP), and extra precision (XP) docking. HTVS docking was performed with a flexible docking algorithm against BT_F392W eliminated zinc compounds that had more than 300 atoms and 50 rotatable bonds. The HTVS docked compounds were filtered based on the Tice rule. The top 10% of compounds based on binding energy from HTVS were docked in the SP mode, and the top10% from SP screening were docked in XP mode. Molecules with the best Glide score and Glide energy were visually inspected and considered for further analysis.

Docking. The top six hits obtained from virtual screening and six known pesticides (discussed earlier) were docked with three wild type and their respective mutant variants. This was done to ensure that the identified compounds have affinity to both the insecticide-susceptible and insecticide-resistant AChE (all three reported mutations).

Stability Analysis of Docked Complexes. The protein target structures (mutated and wild type) were simulated as mentioned earlier. The simulation of docked complexes was performed as follows. One compound (identified from virtual screening studies) having a good affinity toward all three known mutations and its respective wild type was taken for further analysis. The complexes involving the identified compound and mutated AChE F392W and wild type were simulated, and the stability was monitored for 100 ns using Gromacs version 4.5.3.

https://doi.org/10.1021/acsomega.1c07359
ACS Omega 2022, 7, 20515−20527

The ligand topology was obtained using Prodrg webserver,[41] and other parameters used were the same as used in the protein simulation discussed above.

RESULT

Data Retrieval. An initial multiple sequence alignment (MSA) of 54 cotton pest AChE sequences helped us in removing duplicates. Thirty-six unique sequences comprise *Aphis gossypii* (12), *Helicoverpa armigera* (7), *Apolygus lucorum* (6), *Lygus Hesperus* (3), *Bemisia tabaci* (3), *Spodoptera littoralis* (2), *Spodoptera exigua* (2), and *Spodoptera litura* (1). These sequences were aligned, and the similarity profile of aligned sequences obtained from Plotcon is shown in Figure 2. It can be seen that higher similarity region was found around ∼260 to ∼510 residues, and the area ∼300−310 and ∼400−420 seems to be relatively divergent.

Phylogenetic Tree. The NJ tree generated by MEGA was analyzed to gather the evolutionary information of the AChE enzyme (Figure 3). The tree has two main clades: AChE1 and AChE2. Both the clades display an aggregation of sequences under their respective species-wise sub-clades involving species *Aphis gossypii*, *H. armigera*, *B. tabaci*, and *A. lucorum*. It could also be understood from the tree that both the AChE1 and AChE2 sequences of *L. hesperus* accommodate themselves in close relationship with *A. lucorum*. From the tree, it is noted that AChE sequences of the same order and species are highly conserved. This provides us the base for developing broad-spectrum pesticides having the potential to inhibit AChE in pests from the same order.

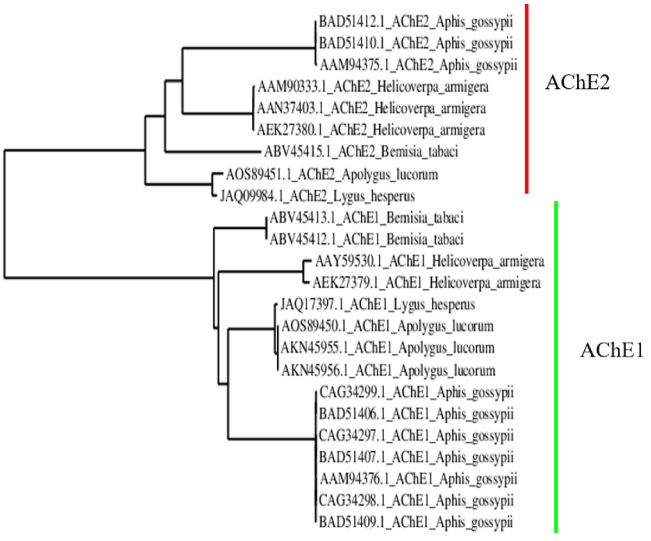

Figure 3. Phylogenetic Tree of AChE. Clade 1 contains AChE2 and clade 2 contains AChE1 sequences.

Primary Sequence Analysis. The length of AChE sequences ranges from 300 to 700 aa. The amino acid composition is represented as a chart in Figure SF1. Physiochemical properties are given in Table ST1. Physiochemical properties showed that negatively charged residues (Asp +Glu) were higher than positively charged residues (Arg + Lys). Hydropathicity (GRAVY) shows that the majority of the sequences are hydrophilic. The average molecular weight of AChE is around 60 kDa. All the sequences contained a motif related to the carboxylesterase family (Figure SF2). Motif profiling was done to ensure that the selected sequences are AChE indeed.

Mutation Analysis. The molecular basis of insects showing resistance to organophosphates, pyrethroids, carbamates, and chlorpyrifos is due to mutations in the insecticidal target site. From the literature, three-point mutations in AChE1 were identified in *A. lucorum* (AOS89450.1, hereafter AL_MT), *B. tabaci* (ABV45412.1, hereafter BT_MT), and *A. gossypii* (BAD51410/BAD51412, hereafter AG_MT) at A216S, F392W, and A302S, respectively, and these details are listed in Table 1.

Stability Analysis of Mutant Proteins. The I-mutant2.0 server predicted the impact of these mutations on enzyme stability. I-mutant calculates the energy difference between native and mutant protein based on Gibbs's free energy.[42] The difference between the unfolding Gibbs free energy value of the mutated protein and wild type (kcal/mol) gives us the DDG value, which measures the effect of single point mutation on protein stability. Protein with a DDG value less than zero will have reduced stability and vice versa. The DDG of AL_MT, BT_MT, and AG_MT is −0.44, −1.37, and −1.13, respectively. BT_MT F392W had a DDG value that was less compared to the other two mutations. Figure 4 shows mutations occurring in sites in different AChE1. Alanine and serine are categorized as less hydrophobic and hydrophilic amino acids, respectively. Figure 4A,B shows that A216S and A302S are on the coil region. Phenylalanine is hydrophobic, and tryptophan is relatively less hydrophobic; this mutation lies in the helix of AChE (Figure 4C).

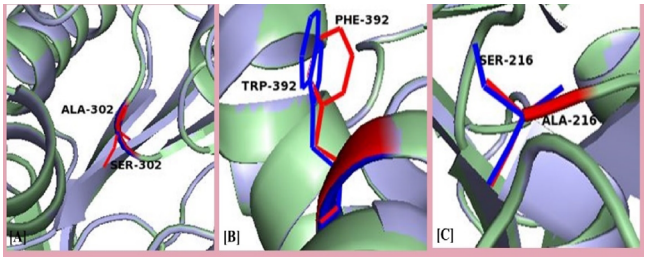

Figure 4. (A) *Aphis gossypii* (A216S), (B) *Apolygus lucorum*, and (C) *Bemisia tabaci* (A302S). Substitution of A to S replaces one of the methylene hydrogens with a hydroxyl group. F and W are derivatives of alanine, F has phenyl substitution, and W has indole substitution in the beta carbon of alanine. Structural differences due to mutation can be noticed.

Molecular Modeling and Validation. The modeled AChE structures were validated by using ERRAT, Verify3D,

Table 1. Mutation Reported in AChE of Different Species

protein ID	gene ID	organism	family	mutation	reference
AOS89450.1	KT805420.1	*Apolygus lucorum*	Miridae	A216S	48
ABV45412.1	EF675187	*Bemisia tabaci*	Aleyrodidae	F392W	49
BAD51410/BAD51412	AB180401, AB180403	*Aphis gossypii*	Aphididae	A302S	47

https://doi.org/10.1021/acsomega.1c07359
ACS Omega 2022, 7, 20515−20527

Table 2. Homology Modeling: Template Details and Validation Report

		template details					RC plot		
query	query organism	PDB ID	query coverage	identity %	verify 3D	ERRATscore	% favored	% allowed	% outlier
AOS89450.1_MT	*Apolygus lucorum*	2W6C_X	90	45	90.96	92.263	94.5	5.1	0.4
AOS89450.1_WT	*Apolygus lucorum*	2W6C_X	90	45	90.96	92.263	94.5	5.1	0.4
ABV45412.1_MT	*Bemisia tabaci*	2W6C_X	82	44	95.51	93.269	94.4	4.9	0.7
ABV45413.1_WT	*Bemisia tabaci*	2W6C_X	82	44	94.57	94.615	94.7	4.3	0.9
BAD51412_MT	*Aphis gossypii*	1DX4_A	81	55	93.98	86.667	94	4.9	1.1
BAD51412_WT	*Aphis gossypii*	1DX4_A	81	55	93.98	86.667	94	4.9	1.1

and Ramachandran (RC) plots. Details of the templates and validation report are shown in Table 2. The ERRAT score of all structures was greater than 80, and in the RC plot, around 98% of the residues were found to be aggregating in the allowed region. This validation confirms that the modeled structures were reliable for further study.

AChE Structural Analysis. The modeled structure of AChE was analyzed with reference to AChE of *Torpedo californica* (PDB ID: 2ACE)[43] to gain knowledge about active sites. The active site of AChE contains two subsites, the (i) esteric site and (ii) anionic site. In the esteric site, the Ser−His−Glu catalytic triad is present.[43,44] This catalytic triad is present at sites 262, 501, and 388 in BT_WT/MT, 276, 521, and 405 in AG_WT/MT and 215, 455, and 341 in AL_WT/MT.

The anionic site is formed by four residues Trp−Tyr−Tyr−Phe.[44] The location of the four-residue anionic site in BT_WT/MT, AG_WT/MT, and AL_WT/MT is 147, 193, 391, and 392; 145, 201, 408, and 409, and 100, 146, 344, and 345, respectively. Other sites present in AChE are the acyl binding pocket, oxyanion hole, and peripheral anionic site (PAS). In BT_MT, Phe at 392 of the anionic site is mutated to Trp. In AL_MT, the Ala residue at the oxyanion hole is mutated to Ser. Cartoon representation of AChE active sites is shown in Figure 5.

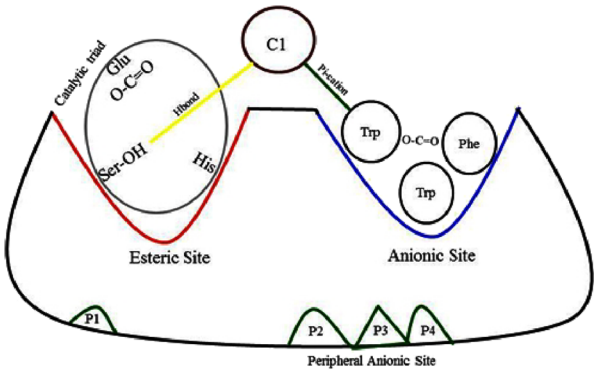

Figure 5. Cartoon Representation of the AChE active pocket.

Molecular Dynamics Based Conformational Flexibility and Stability Analysis. I-Mutant2.0 server predicts the change in free energy change. DDG greater than or equal to zero indicates the higher stability of the mutant protein.[33] The F392W mutation has higher negative DGG than others and, therefore, is known to decrease the stability of the protein. So, the structural and functional behavior of wild and mutant (F392W) AChE was studied using the Gromacs MDS package for a period of 100 ns.

Potential Energy. The potential energy observed during the simulation plotted against time is shown in Figure 6. From the figure, it can be seen that both the systems have stable energy throughout the simulation. The average potential energy reported by wild type protein was −1,316,214 KJ/mol, and the mutant was −1,310,308 KJ/mol. The overall difference in energy between the two types is around 600 KJ/mol. As stated earlier, the simulation confirms that both the systems have attained equilibrium and, therefore, can act as a reference for our further similar study involving docked complexes.

RMSD of Protein. Global changes in the protein structure upon mutation were monitored as a function of RMSD plotted against time. The backbone RMSD profile is shown in Figure 7. The wild type AChE and mutant AChE-F392W structure reached equilibrium after 30 ns. Approximately, after 70 ns, the systems were more converged, and very minor fluctuations were noted in mutant protein at 85 to 90 ns. This minor deviation reflects the changes in protein stability upon amino acid substitution. Also evident from the figure is that RMSD was higher in AChE than AChE-F392W. The maximum RMSD was around 0.37 and 0.35 nm for wild and mutant types, respectively.

C-Alpha RMSF and Radius of Gyration. The wild and mutant AChE showed different fluctuation patterns, and the mutation induced changes in the flexibility of the protein, indicating that the mutation may affect the function of the protein. The RMSF fluctuation centered around the mutated residue, as shown in Figure 8, emphasizes a similar trajectory in both the mutant and wild type AChE. The radius of gyration (R_g) chart of wild and mutant AChE against time is shown in Figure 9. It can be seen that the wild type and mutant AChE were compact throughout the simulation. The average R_g values of wild type and mutant AChE were 2.27 and 2.43 nm, respectively. This also suggests that wild type AChE is more compact, and the increased R_g in mutant type AChE could loosen the active pocket, which makes the inhibitor molecule bind on the surface instead of deep inside the binding pocket, leading to unstable interaction as shown in Figure 11.

Hydrogen Bonding. One of the main factors responsible for maintaining protein structure stability is hydrogen bonds.[42] Analyzing the number of hydrogen bonds in wild type and mutant AChE proteins is essential to understand the stability between the residues in these proteins. The intramolecular hydrogen bond is shown in Figure 10. During the final 10 ns, wild and mutant AChE formed a maximum of 370−432 and 364−434 hydrogen bonds, respectively. The average hydrogen bonds observed were 400.63 and 398.86, respectively. Hydrogen bond counts varied in the mutant compared with the wild type AChE. The change in hydrogen bond counts depicts the power of deleterious amino acid in H-bond formation.

Principal Component Analysis. Essential dynamics was used for a border view of dynamic properties with respect to MDS results. The projection of the first two eigenvectors for wild type and mutant AChE is shown in Figure 12. The covariance matrices of C-alpha atoms for wild type and mutant AChE were 14.78 and 9.97 nm^2 respectively. The covariance

https://doi.org/10.1021/acsomega.1c07359
ACS Omega 2022, 7, 20515−20527

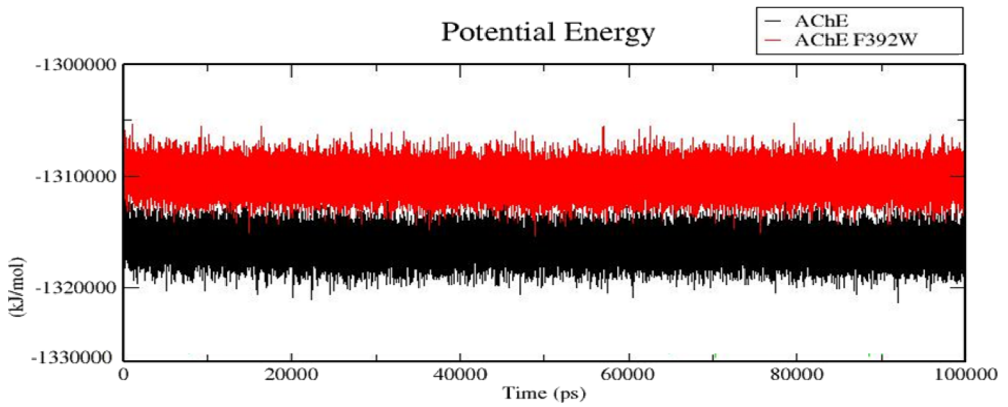

Figure 6. Potential energy of the systems plotted against time. Black and red lines indicate the potential energy of the AChE wild type and AChE mutant type.

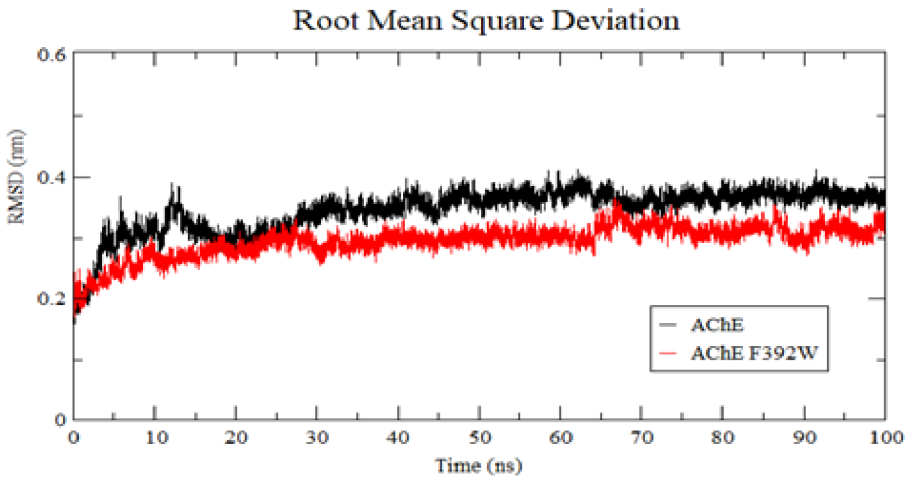

Figure 7. Backbone RMSD of the protein structures. The *X*-axis is RMSD (nm), and the *Y*-axis is time (ns). Black and red lines indicate the RMSD of the AChE wild type and AChE mutant type, respectively.

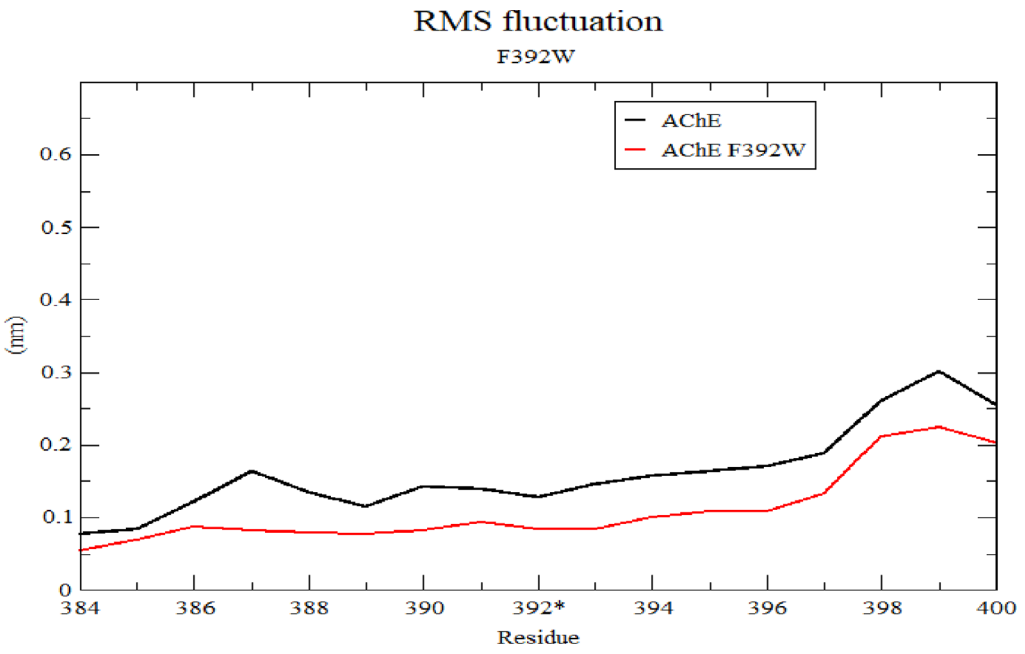

Figure 8. RMSF profile of around the mutant site F392W.

https://doi.org/10.1021/acsomega.1c07359
ACS Omega 2022, 7, 20515−20527

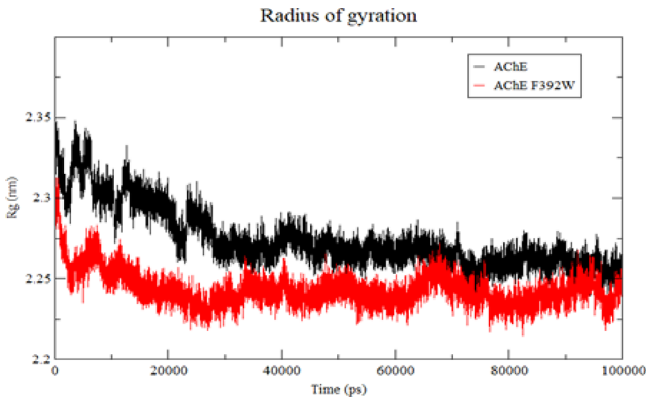

Figure 9. Radius of gyration of the protein structures. The *X*-axis is RMSD (nm), and the *Y*-axis is time (ns). Black and red lines indicate the RMSD of AChE wild type and AChE mutant type, respectively.

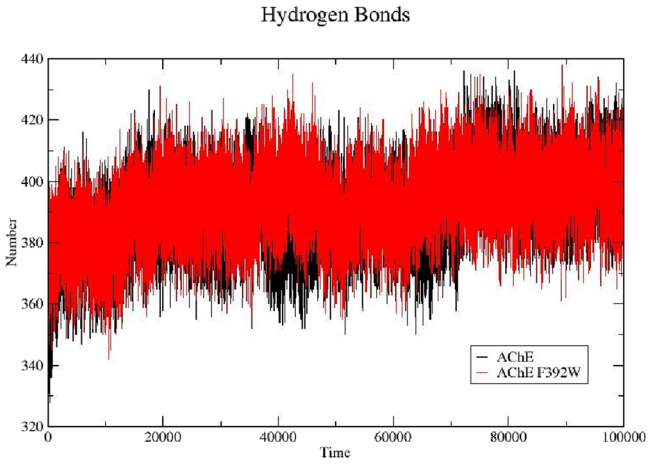

Figure 10. Intramolecular hydrogen profile of the wild and mutant AChE proteins. The *X*-axis is time in ps, and the *Y*-axis is the hydrogen bond count. Black lines: AChE wild type; red lines: AChE mutant type.

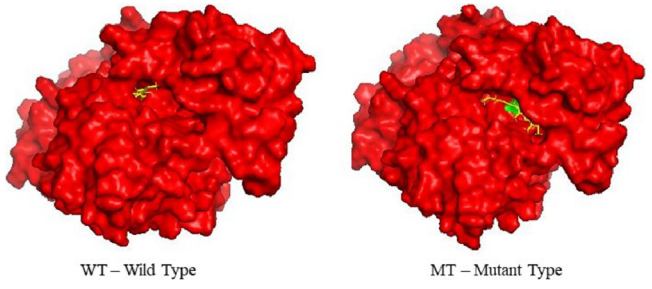

Figure 11. Surface model of AChE wild and mutant structures showing change in the binding pocket. Red: AChE; yellow: pesticide. In the wild type, the inhibitor molecule is bound deep inside the groove, and in the mutant type, the structure of groove was altered and inhibitor lies on the surface of the molecule.

matrix of C-alpha atoms for wild AChE was higher compared to the mutant. The projection of the first two eigenvectors in phase space for wild type and mutant AChE explained that the cluster of the wild type is stable, and in mutant AChE, it is expanded in the conformational space due to flexibility.

Virtual Screening. Pesticide-like compounds having a binding affinity towards wild and mutant AChE were predicted using the computer-aided pesticide designing approach. The grid of mutant BT_W392F was used for virtual screening against

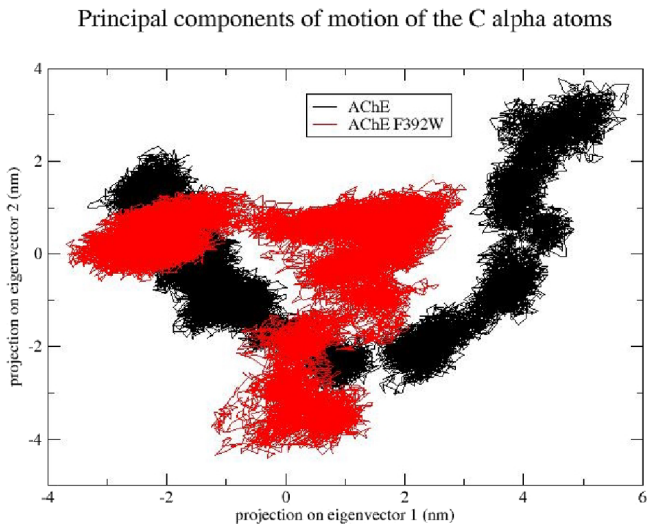

Figure 12. Principal component analysis. Black and red lines indicate AChE wild type and AChE mutant type, respectively.

the ZINC natural database in hierarchical mode (HTVS → SP → XP).[45] Tice rule and a three-tier virtual screening protocol (HTVS, SP, and XP) resulted in 39,086 compounds with a binding energy ranging from 4.45 to −10.18 kcal/mol. The top 10 % of HVTS compounds were docked in the SP mode. The SP docked compounds have a binding energy between −1.77 and −10.59 kcal/mol, and finally, 391 SP docked compounds were passed to XP docking, and XP docking resulted in a glide score ranging between −8.46 and −13.11 kcal/mol.

Docking. The selected hits from the virtual screening study were re-docked to reaffirm the binding affinity of the compounds toward BT_F392W AChE. The binding energy between AChE and inhibitor molecules and residues involved in forming hydrogen bonds is shown in Table 3. Residues Tyr184, Gly182,

Table 3. Binding Energy Details of AChE with Identified Compounds

compound	dock score	energy (kcal/mol)	H-bond	pi−pi stacking
ZINC95099639	−13.11	−31.96	Tyr184, Gly180	Trp147
ZINC03812983	−11.98	−33.84	Ser262, Gly182, Glu261	Trp392
ZINC95099641	−12.11	−35.56	Asn148	Trp147
ZINC70455604	−12.49	−37.56	No	No
ZINC32273181	−12.27	−34.97	Thr185	Trp147
ZINC95098859	−12.12	−32.42	Gly180, Tyr391	Trp147

Thr185, Ser262, Asn148, and Glu261 are engaged in H-bond interaction. Trp147 and Trp392 were involved in pi−pi stacking. The compound ZINC95099639 has less binding energy with two hydrogen bonds, and the compound ZINC03812983 has a maximum of three hydrogen bonds with a binding energy of −11.98 kcal/mol. ZINC70455604 has a binding energy of −12.48 kcal/mol with no hydrogen bond interaction with AChE. Figure 13 shows the binding pocket residues of AChE and the residues involved in the interaction with ligand molecules.

Docking with Known and Identified Pesticides. Six known pesticides and six identified compounds were docked to the wild and mutant structures of AL_MT, BT_MT, and AG_MT. The binding energy between the compounds (known

https://doi.org/10.1021/acsomega.1c07359
ACS Omega 2022, 7, 20515−20527

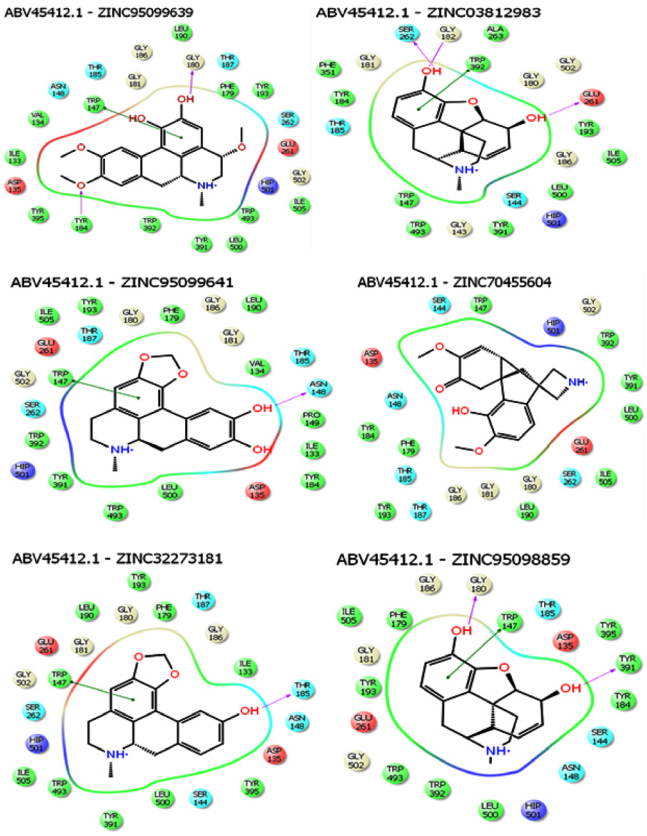

Figure 13. Binding mode interaction of BT_MT with identified compounds. Green: hydrophobic; purple: charged (positive); cyan: polar; yellow: glycine; orange: hydration set; green line: pi−pi stacking; arrow (purple): backbone H-bond; dotted arrow (purple): side chain H-bond.

pesticide and identified) and AChE (wild type and mutant) is shown in Table 4. Details of residues involved in hydrogen bond interactions are shown in Table ST2. We found that compound ZINC03812983 had an excellent affinity toward the resistant and susceptible AChE followed by ZINC95098859, ZINC95099641, and others. Only ZINC03812983 (C1) binds to the serine residue present in the catalytic triad of AChE, which is a critical residue in the inhibition of AChE by phosphorylating or carbamylating it. This compound was taken for molecular dynamics study. The interaction of C1 with wild type and susceptible AChE is shown in Figure 14. The Tice rule property of the identified compounds is shown in Table 5.

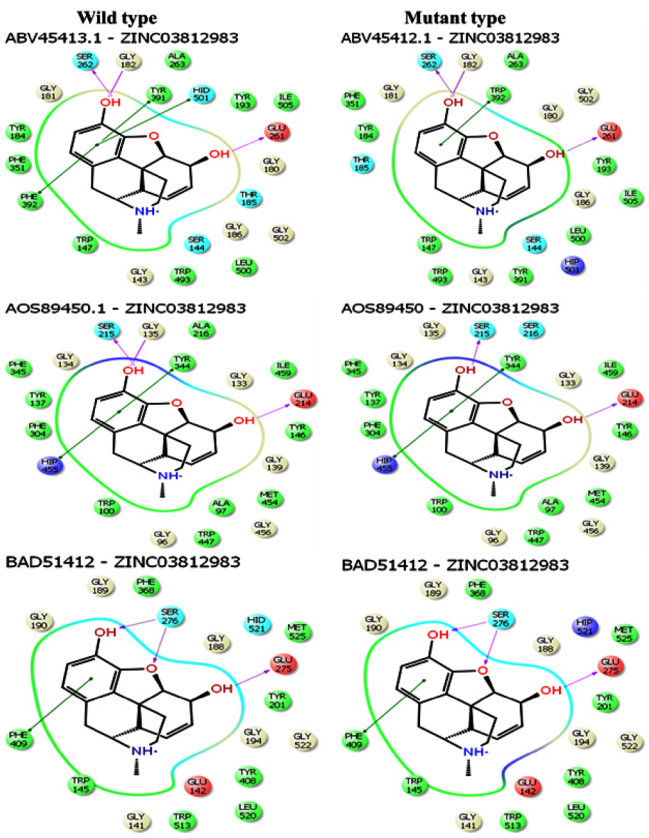

Figure 14. Binding mode interaction of C1 with wild type and mutant protein. Green: hydrophobic; purple: charged (positive); cyan: polar; yellow: glycine; orange: hydration set; green line: pi−pi stacking; arrow (purple): H-bond backbone; dotted arrow (purple): side chain H-bond.

Molecular Dynamics Simulation of Docked Complex.

The ZINC compound ZINC03812983 (hereafter referred to as C1) is predicted to have a good affinity toward AChE of both the insecticide-susceptible and insecticide-resistant insects. The stability of the docked complex of wild AChE-C1 and mutant AChE F392W-C1 was studied for 100 ns using Gromacs and molecular dynamics simulation package. The potential energy of

Table 4. Binding Energy Interaction between Native and Mutant ACHE1 and Compounds[a]

protein/ compounds	ABV45412 (MT) (kcal/mol)	ABV45413 (WT) (kcal/mol)	AOS89450 (MT) (kcal/mol)	AOS89450 (WT) (kcal/mol)	BAD51412 (MT) (kcal/mol)	BAD51412 (WT) (kcal/mol)
chlorpyrifos	−4.63	−4.49	−5.45	−6.36	−5.56	−6.43
malathion	−4.39	−4.61	−4.96	−4.78	−5.45	−6.67
acephate	−3.02	−3.33	−3.46	−3.81	−4.03	−4.28
methomyl	−2.50	−2.92	−3.00	−3.10	−3.13	−3.29
thiodicarb	−1.34	−3.21	−3.21	−3.60	−4.00	−3.06
deltamethrin	−5.47	−6.84	−7.72	−6.86	−10.27	−9.39
ZINC95099639	−13.11	−8.06	NA	NA	NA	−5.71
ZINC03812983[a]	−12.50	−11.23	−9.91	−9.93	−9.85	−11.69
ZINC70455604	−12.49	−8.35	−9.03	−8.70	−5.86	−7.37
ZINC95098859	−12.41	−9.51	−8.11	−9.58	−8.60	−11.59
ZINC32273181	−12.28	−9.06	−6.95	−10.21	−10.36	−9.18
ZINC95099641	−12.11	−7.68	−11.10	−10.18	−9.29	−14.73

[a]*, best compound; NA, no interaction observed; MT, mutant type; WT, wild type.

https://doi.org/10.1021/acsomega.1c07359
ACS Omega 2022, 7, 20515−20527

Table 5. Tice Pesticide-like Properties of the Compounds[a]

compound	name	*x*log*P*	H-bond donors (HBD)	H-bond acceptors (HBA)	molecular weight (MW)	rotatable bonds (RB)
ZINC95099639	4*S*-methoxylastourvilline	2.25	2	6	357.40	3
ZINC03812983	(−)-heroin hydrochloride	1.1	3	4	286.35	0
ZINC70455604	hydroxy-dimethoxy-methyl-BLAHone	0.57	2	5	328.38	2
ZINC95099641	10-*O*-demethylcassythicine	4.26	3	5	312.34	0
ZINC95098859	morphine	1.1	3	4	286.35	0
ZINC32273181	mecambroline	3	2	4	296.34	0

[a]Tice pesticide-likeliness property: molecular weight = 150−500, hydrogen bond donor = ≤2, hydrogen bond acceptor = 1−8, rotatable bonds = <12.[40]

both the systems was stable throughout the simulation (Figure 15). The highest and lowest potential energies observed over 100 ns for AChE-C1 were −1,339,649 and 1,329,997 kJ/mol, and those for AChE-F392W-C1 were −1,338,953 and −1,327,752 kJ/mol, respectively. The average potential energies for AChE-C1 and AChE-F392W-C1 were −1,334,895 and −1,333,687 kJ/mol. The average RMSD values of AChE-C1 and AChE-F392W-C1 were 0.25 and 0.39 nm, respectively (Figure 16). AChE-C1 has low RMSD, this system was well equilibrated after 70 ns, and the AChE-F392W-C1 has minor insignificant fluctuations after 80th ns.

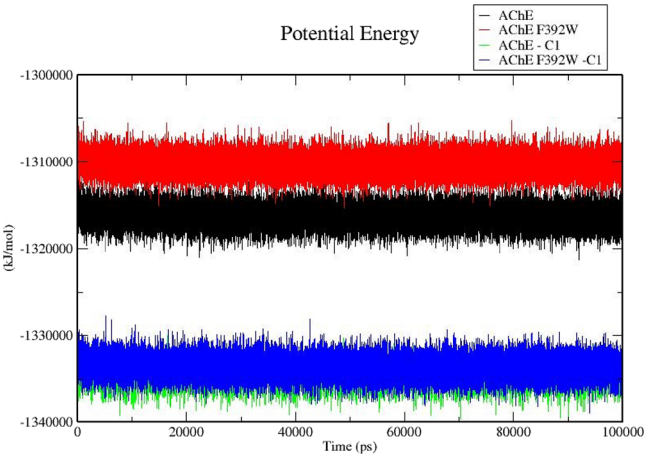

Figure 15. Potential energy of the systems plotted against time. Black, red, blue, and green lines indicate the potential energy of AChE wild type, AChE mutant type, AChE wild type bound with identified inhibitor C1, and AChE mutant type bound with identified inhibitor C1, respectively.

The RMSF fluctuations of residues surrounding mutation F392W is shown in Figure 17. From the plot, it can be seen that native AChE has a higher RMSF profile compared to other systems. The RMSF profile of the system changes upon C1 binding, which may result in the loss of function. The radius of gyration is a way to measure the compactness of the system throughout the simulation. The graph shown in Figure 18 shows the compactness of the protein analyzed from the 100 ns trajectory. The average R_g values observed throughout the simulation were 2.26 and 2.28 nm. A maximum of four and seven hydrogen bonds were observed between AChE and C1 and AChE F392W and C1 throughout the simulation, respectively. Molecular dynamics analysis indicates the strong interaction between AChE and the compound C1.

Solvent Accessible Surface Area. The solvation effect is another crucial factor that helps to maintain protein stability and

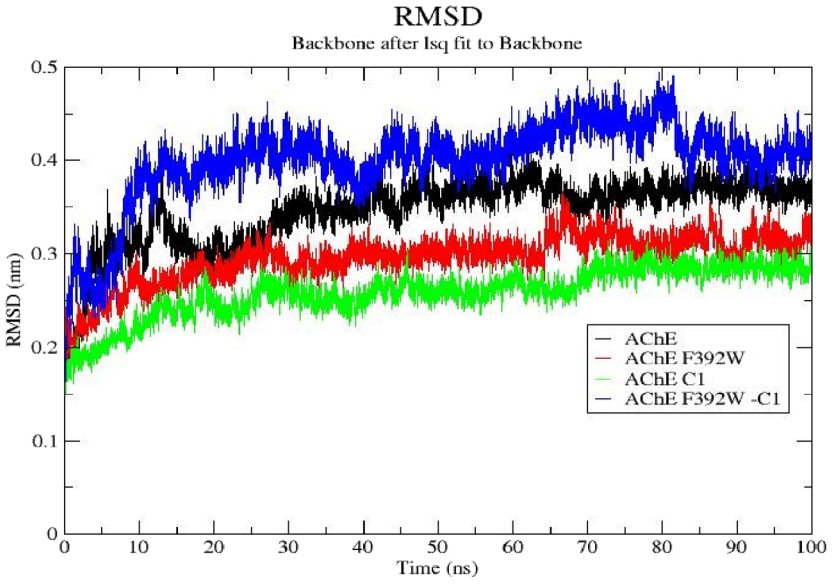

Figure 16. Backbone RMSD of the protein structures. The *X*-axis is RMSD (nm), and the *Y*-axis is time (ns). Black, red, blue, and green lines indicate the RMSD of AChE wild type, AChE mutant type, AChE wild type bound with identified inhibitor C1, and AChE mutant type bound with identified inhibitor C1, respectively.

https://doi.org/10.1021/acsomega.1c07359
ACS Omega 2022, 7, 20515−20527

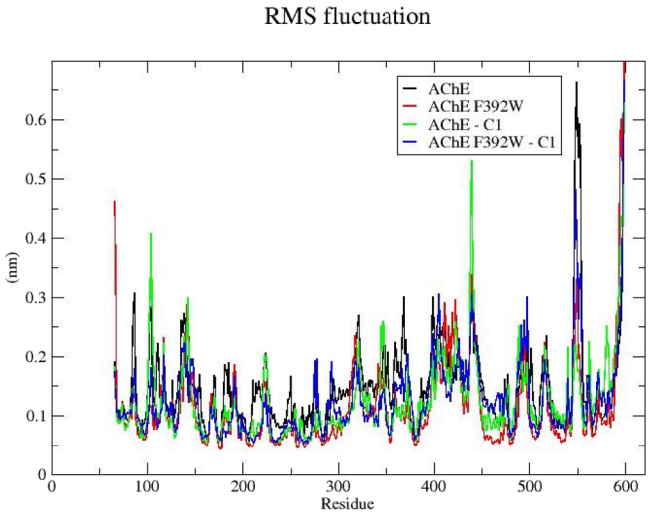

Figure 17. Central alpha-carbon RMSF of the wild type and mutant AChE proteins. The *X*-axis is the residue position, and the *Y*-axis is RMSF (nm). Black, red, blue, and green lines indicate the RMSF of AChE wild type, AChE mutant type, AChE wild type bound with identified inhibitor C1, and AChE mutant type bound with identified inhibitor C1, respectively.

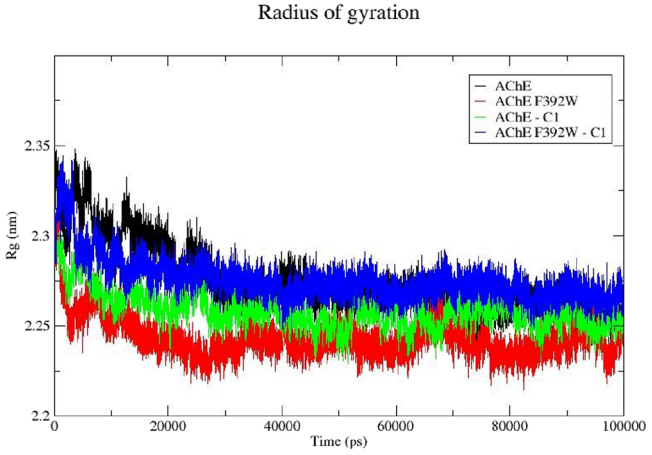

Figure 18. Radius of gyration (R_g) of the wild and mutant AChE proteins. The *X*-axis is time in (ps), and the *Y*-axis is R_g (nm). Black, red, blue, and green lines indicate the R_g of AChE wild type, AChE mutant type, AChE wild type bound with identified inhibitor C1, and AChE mutant type bound with identified inhibitor C1, respectively.

folding.[42] Changes in the solvent-accessible surface area of wild and mutant AChE with respect to time are shown in Figure 19. The average SASA values exhibited by wild and mutant proteins were 224.40 and 219.60 nm^2, respectively. The mutant protein showed a relatively lower SASA than the wild type, which indicates the repositioning of amino acids from buried to the accessible area or vice versa.

DISCUSSION

Acetylcholinesterase (EC: 3.1.1.7) coded by Ace gene is a crucial enzyme that regulates the neurotransmitter acetylcholine and terminates nerve impulses. Acetylchonline (Ach) is an important neurotransmitter that gets hydrolyzed by AChE at cholinergic synapses, making AChE critical for the normal functioning of the central nervous system.[46] Two main classes of

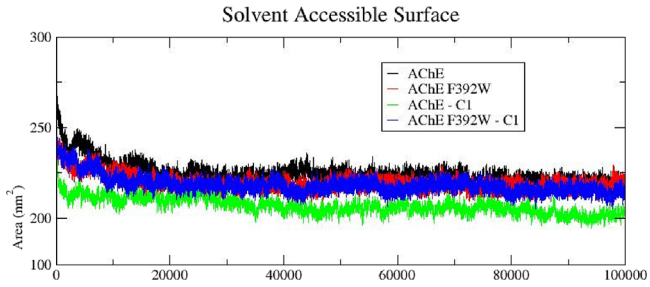

Figure 19. Solvent accessible surface area. The *X*-axis is time in ps, and the *Y*-axis is area in nm^2. Black, red, blue, and green lines indicate the SASA of AChE wild type, mutant type, wild type bound with identified inhibitor C1, and mutant type bound with identified inhibitor C1, respectively.

pesticide, namely, organophosphates and carbamate, are known to target AChE.[47]

In the current study, existing AChE sequences of eight cotton pests, which include four species from Hemiptera and four from Lepidoptera, were studied. Phylogenetic analysis of these sequences revealed that the AChE sequence maintained similarity across order and species. Since the AChE sequence is conserved across order (taxonomy level), designing a new class of pesticide (AChE inhibitor) will help control cotton pests of the order Hemiptera. The average sequence length of AChE is around 542 amino acids. Literature survey-based mutation analysis led us to understand three point mutations *Bemisia tabaci* F392W, *Aphis gossypii* A302S, and *Apolygus lucorum* A216S. These three mutations resulted in the shifting of amino acids from hydrophobic to the hydrophilic core, and this might have an impact in the solvent-accessible surface area. Structural analysis of AChE revealed two important subsites in the AChE catalytic site: (i) the esteric site possesses the active OH of serine, imidazole of histidine, and the COO− group of glutamate.[46] These three residues (Ser−His−Glu) form a catalytic triad in which the organophosphates are known to react with serine.[43] (ii) The anionic site is a choline-binding pocket, and it is believed to be a binding site for competitive inhibitors containing the free carboxyl (Asp/Glu) group,[44,46] TRP, TYR, TYR, and PHE. Choline moiety binds to the anionic site mainly through pi−cation interaction.[44]

Conformational flexibility of the wild type and mutant AChE was studied using Gromacs. RMSD, RMSF, hydrogen bonding, R_g, and SASA trajectories were plotted against time. Both systems have stable potential energy throughout the simulation. The C-alpha amino acid fluctuation reflects the changes in the flexibility of AChE upon mutation (F392W). Principal component analysis of the wild type and mutant F392W AChE also portrayed the impact of this mutation.

Computer-aided pesticide design was carried out to identify compounds having the ability to inhibit AChE of insecticide-resistant and insecticide-susceptible pests. Virtual screening exercise resulted in compounds having an affinity toward AChE. Six compounds identified from the virtual screening study along with six known pesticides were considered for checking their affinity toward AChE from insecticide-resistant and insecticide-susceptible insects. Based on docking studies, ZINC03812983 (C1) is found to have excellent affinity compared to available pesticides. Interaction analysis of C1with mutant and wild type AChE shows that the identified compound C1 binds at the active site of AChE and the OH at the benzene ring forms a hydrogen bond with the Ser262 residue of the catalytic triad.

https://doi.org/10.1021/acsomega.1c07359
ACS Omega 2022, 7, 20515−20527

The compound was found to bind in the deep groove of AChE. This compound also forms pi−cation interaction with Trp392, which was a mutant residue (BT_F392W). C1 also binds well with other mutant and wild type proteins and forms a hydrogen bond and pi−cation interaction with serine of the catalytic triad and phenylalanine, respectively. This confirms that the identified compound can bind to AChE of insecticide-susceptible and insecticide-resistant insects. The identified compounds can be taken for further chemical synthesis leading to advanced in vitro and in vivo assessment and product development.

CONCLUSIONS

Economically important cotton fiber produced by Gossypium spp. is affected by thousands of pests, which have evolved pesticide resistance to a wide range of pesticides. Mutation in the target's active site of enzymes such as AChE is attributed to insects developing resistance. In this study, AChE sequences from major pests of cotton were analyzed for its prevalence in these pests and we found AChE1 and AChE2 to be present. Reported mutations in AChE1 were selected, and their impact on the structural and functional properties of AChE1 was studied. We chose F392W_AChE1 and wild type AChE1 for the virtual screening and SP and XP docking of zinc natural compounds. Six compounds from the screening and six known pesticides were further docked with three mutant and three wildt ype AChE1 to select a compound ZINC03812983 (C1) that satisfied the Tice rule and also had binding affinity to the mutant and wild type. A further molecular dynamics simulation of the F392W_AChE1-C1 and wild type AChE1-C1 complexes demonstrated C1 to have firmly bound to both the AChE1 types and displayed acceptable thermodynamic properties and conformational stabililty. Therefore, we believe that C1 has the pesticide-like property and could impact both the insecticide-susceptible and insecticide-resistant species. Further studies such as synthesis and field testing of C1 on different cotton pests are needed and could be taken up as an extension of this study to understand the potential and efficacy.

ASSOCIATED CONTENT

Supporting Information

The Supporting Information is available free of charge at https://pubs.acs.org/doi/10.1021/acsomega.1c07359.

(Figure SF1) Amino acid composition of AChE sequences; (Figure SF2) MOTIFs present in AChE sequences identified by MEME Suite; (Table ST1) physiochemical properties of AChE sequences; and (Table ST2) interacting residues of AChE with known and identified compounds (PDF)

AUTHOR INFORMATION

Corresponding Author

Habeeb Shaik Mohideen − *Bioinformatics and Entomoinformatics Lab, Department of Genetic Engineering, School of Bioengineering, College of Engineering and Technology, SRM Institute of Science and Technology, Chennai, Tamilnadu 603203, India;* orcid.org/0000-0003-4217-5063; Email: habeeb_skm@yahoo.co.in, habeebm@srmist.edu.in

Authors

Seethalakshmi Sakthivel − *Bioinformatics and Entomoinformatics Lab, Department of Genetic Engineering, School of Bioengineering, College of Engineering and Technology, SRM Institute of Science and Technology, Chennai, Tamilnadu 603203, India*

Chandrasekar Raman − *Lab Manager, Integrative Physiology & Metabolism, Joslin Diabetes Center, Harvard Medical School, Boston, Massachusetts 02215, United States*

Saharuddin Bin Mohamad − *Institute of Biological Sciences, Faculty of Science, Universiti Malaya, Kuala Lumpur 50603, Malaysia*

Complete contact information is available at: https://pubs.acs.org/10.1021/acsomega.1c07359

Notes

The authors declare no competing financial interest.

ACKNOWLEDGMENTS

The authors are thankful to Department of Biotechnology, New Delhi, India, for providing financial assistance through Bioinformatics National Certification (BINC) fellowship (fellow no. DBT-BINC/2017/SRM/8), DST-SERB (grant no. YSS/2014/000293) for partial funding support, and High Performance Computing Center, SRM Institute of Science and Technology for providing the computational facility.

REFERENCES

(1) Thrall, P. H.; Bever, J. D.; Burdon, J. J. Evolutionary change in agriculture: The past, present and future. *Evol. Appl.* **2010**, *3*, 405−408.

(2) Mollaee, M.; Mobli, A.; Mutti, N. K.; Manalil, S.; Chauhan, B. S. Challenges and Opportunities in Cotton Production. In *Cotton Production*, 1st ed.; Jabran, K.; Chauhan, B. S. Wiley-Blackwell: UK, 2019; pp. 371−390.

(3) *Cotton Corporation of India*. https://cotcorp.org.in/national_cotton.aspx. Accessed on Sep, 16 2020.

(4) Kevan, P. G.; Shipp, L. Biological Control as Biotechnological Amelioration and Ecosystem Intensification in Managed Ecosystems. In *Reference Module in Life Sciences* (Elsevier, 2017). DOI: 10.1016/b978-0-12-809633-8.09246-3.

(5) Sidhu, G. K.; Singh, S.; Kumar, V.; Dhanjal, D. S.; Datta, S.; Singh, J. Toxicity, monitoring and biodegradation of organophosphate pesticides: A review. *Crit. Rev. Environ. Sci. Technol.* **2019**, *49*, 1135−1187.

(6) Luo, S.; Naranjo, S. E.; Wu, K. Biological control of cotton pests in China. *Biol. Control.* **2014**, *68*, 6−14.

(7) Jackson, C. J.; Liu, J. W.; Carr, P. D.; Oakeshott, J. G. Structure and function of an insect α -carboxylesterase (αEsterase7) associated with insecticide resistance. *PNAS* **2013**, *110*, 10177−10182.

(8) Li, C.; Guo, X.; Zhang, Y.; Dong, Y.; Xing, D.; Yan, T.; Wang, G.; Zhang, H.; Zhao, T. Identification of genes involved in pyrethroid- , propoxur- , and dichlorvos- insecticides resistance in the mosquitoes , *Culex pipiens* complex (Diptera : Culicidae). *Acta Trop.* **2016**, *157*, 84−95.

(9) Li, Y.; Farnsworth, C. A.; Coppin, C. W.; Teese, M. G.; Liu, J.; Scott, C.; Zhang, X.; Russell, R. J.; Oakeshott, J. G. Organophosphate and Pyrethroid Hydrolase Activities of Mutant Esterases from the Cotton Bollworm *Helicoverpa armigera*. *PLoS One* **2013**, *8*, No. e77685.

(10) Yu, Q.-Y.; Lu, C.; Li, W.-L.; Xiang, Z.-H.; Zhang, Z. Annotation and expression of carboxylesterases in the silkworm. *BMC Genomics* **2009**, *10*, 553.

(11) Colovic, M. B.; Krstic, D. Z.; Lazarevic-Pasti, T. D.; Bondzic, A. M.; Vasic, V. M. Acetylcholinesterase Inhibitors: Pharmacology and Toxicology. *Curr. Neuropharmacol.* **2013**, *11*, 315−335.

(12) Labbé, P.; Alout, H.; Djogbénou, L.; Pasteur, N.; Weill, M. G. Evolution of Resistance to insecticide in disease vectors. In *Genetics and Evolution of Infectious Diseases*. Elsevier: UK, 2011, pp. 363−409. DOI: 10.1016/B978-0-12-384890-1.00014-5.

(13) Lokeshwari, D.; Krishna Kumar, N. K.; Manjunatha, H. Multiple Mutations on the Second Acetylcholinesterase Gene Associated With Dimethoate Resistance in the Melon Aphid , *Aphis gossypii* (Hemiptera : Aphididae). *J. Econ. Entomol.* **2016**, *109*, 887−897.
(14) *Goal 2: Zero hunger | UNDP*. https://www.undp.org/content/undp/en/home/sustainable-development-goals/goal-2-zero-hunger.html. *Accessed on Sep, 16 2020.*
(15) Gahukar, R. T. Potential and Utilization of Plant Products in Pest Control. In *Integrated Pest Management: Current Concepts and Ecological Perspective*. Elsevier: UK, 2014; pp. 125−139.
(16) Ramalho, T. C.; de Castro, A. A.; Silva, D. R.; Silva, M. C.; Franca, T. C. C.; J Bennion, B.; Kuca, K. Computational Enzymology and Organophosphorus Degrading Enzymes: Promising Approaches Toward Remediation Technologies of Warfare Agents and Pesticides. *Curr. Med. Chem.* **2016**, *23*, 1041−1061.
(17) Correy, G. J.; Zaidman, D.; Harmelin, A.; Carvalho, S.; Mabbitt, P. D.; Calaora, V.; James, P. J.; Kotze, A. C.; Jackson, C. J.; London, N. Overcoming insecticide resistance through computational inhibitor design. *Proc. Natl. Acad. Sci. U. S. A.* **2019**, *116*, 21012−21021.
(18) Bu, C.; Peng, B.; Cao, Y.; Wag, X.; Chen, Q.; Li, J.; Shi, G. Novel and selective acetylcholinesterase inhibitors for Tetranychus cinnabarinus (Acari: Tetranychidae). *Insect Biochem. Mol. Biol.* **2015**, *66*, 129−135.
(19) Zhang, A.; Mu, Y.; Wu, F. An enantiomer-based virtual screening approach: Discovery of chiral organophosphates as acetyl cholinesterase inhibitors. *Ecotoxicol. Environ. Saf.* **2017**, *138*, 215−222.
(20) Lee, S.; Barron, M. G. Development of 3D-QSAR model for acetylcholinesterase inhibitors using a combination of fingerprint, molecular docking, and structure-based pharmacophore approaches. *Toxicol. Sci.* **2015**, *148*, 60−70.
(21) Lee, S.; Barron, M. G. A mechanism-based 3D-QSAR approach for classification and prediction of acetylcholinesterase inhibitory potency of organophosphate and carbamate analogs. *J. Comput.-Aided Mol. Des.* **2016**, *30*, 347−363.
(22) Reyes-Espinosa, F.; Méndez-Álvarez, D.; Pérez-Rodriguez, M.; Herrera-Mayorga, V.; Juárez-Salvidar, A.; Cruz-Hernández, M. A.; Rivera, G. In Silico Study of the Resistance to Organophosphorus Pesticides Associated with Point Mutations in Acetylcholinesterase of Lepidoptera: *B. mandarina*, *B. mori*, *C. auricilius*, *C. suppressalis*, *C. pomonella*, *H. armigera*, *P. xylostella*, *S. frugiperda*, and *S. litura*. *Int. J. Mol. Sci.* **2019**, *20*, 2404.
(23) Niraj, R. R. K.; Saini, V.; Kumar, A. QSAR analyses of organophosphates for insecticidal activity and its in-silico validation using molecular docking study. *Environ. Toxicol. Pharmacol.* **2015**, *40*, 886−894.
(24) Loza-Mejía, M.; Salazar, J.; Sánchez-Tejeda, J. In silico studies on compounds derived from calceolaria: Phenylethanoid glycosides as potential multitarget inhibitors for the development of pesticides. *Biomolecules* **2018**, *8*, 121.
(25) Shahbaaz, M.; Kanchi, S.; Sabela, M.; Bisetty, K. Structural basis of pesticide detection by enzymatic biosensing: a molecular docking and MD simulation study. *J. Biomol. Struct. Dyn.* **2018**, *36*, 1402−1416.
(26) Sindhu, T.; Venkatesan, T.; Prabhu, D.; Jeyakanthan, J.; Gracy, G. R.; Jalali, S. K.; Rai, A. Insecticide-resistance mechanism of *Plutella xylostella* (L.) associated with amino acid substitutions in acetylcholinesterase-1: A molecular docking and molecular dynamics investigation. *Comput. Biol. Chem.* **2018**, *77*, 240−250.
(27) Sharma, A. K.; Gaur, K.; Tiwari, R. K.; Gaur, M. S. Computational interaction analysis of organophosphorus pesticides with different metabolic proteins in humans. *J. Biomed. Res.* **2011**, *25*, 335−347.
(28) Kumar, S.; Stecher, G.; Tamura, K. MEGA7: Molecular Evolutionary Genetics Analysis Version 7.0 for Bigger Datasets. *Mol. Biol. Evol.* **2016**, *33*, 1870−1874.
(29) Schwede, T.; Kopp, J.; Guex, N.; Peitsch, M. C. SWISS-MODEL: An automated protein homology-modeling server. *Nucleic Acids Res.* **2003**, *31*, 3381−3385.
(30) Lovell, S. C.; Davis, I. W.; Arendall, W. B., III; de Bakker, P. I.; Word, J. M.; Prisant, M. G.; Richardson, J. S.; Richardson, D. C. Structure validation by Calpha geometry: phi,psi and Cbeta deviation. *Proteins.* **2003**, *50*, 437−450.
(31) Gasteiger, E.; Hoogland, C.; Gattiker, A.; Duvaud, S.; Wilkins, M. R.; Appel, R. D.; Bairoch, A. Protein Identification and Analysis Tools on the ExPASy Server. In *The Proteomics Protocols Handbook. Springer Protocols Handbooks*; Humana Press: USA., 2005, 571−607.
(32) Bailey, T. L.; Boden, M.; Buske, F. A.; Frith, M.; Grant, C. E.; Clementi, L.; Ren, J.; Li, W. W.; Noble, W. S. MEME SUITE: tools for motif discovery and searching. *Nucleic Acids Res.* **2009**, *37*, W202−W208.
(33) Capriotti, E.; Fariselli, P.; Casadio, R. I-Mutant2.0 : predicting stability changes upon mutation from the protein sequence or structure. *Nucleic Acids Res.* **2005**, *33*, 306−310.
(34) Berendsen, H. J. C.; Postma, J. P. M.; Van Gunsteren, W. F.; Dinola, A.; Haak, J. R. Molecular dynamics with coupling to an external bath. *J. Chem. Phys.* **1984**, *81*, 3684−3690.
(35) Essmann, U.; Perera, L.; Berkowitz, M. L.; Darden, T.; Lee, H.; Pedersen, L. G. A smooth particle mesh Ewald method. *J. Chem. Phys.* **1995**, *103*, 8577−8593.
(36) Ryckaert, J. P.; Ciccotti, G.; Berendsen, H. J. C. Numerical integration of the cartesian equations of motion of a system with constraints: molecular dynamics of n-alkanes. *J. Comput. Phys.* **1977**, *23*, 327−341.
(37) Sakthivel, S.; Habeeb, S. K. M.; Raman, C. Screening of broad spectrum natural pesticides against conserved target arginine kinase in cotton pests by molecular modeling. *J. Biomol. Struct. Dyn.* **2019**, *37*, 1022−1042.
(38) Kutzner, C.; Pall, S.; Fechner, M.; Esztermann, A.; de Groot, B. L.; Grubmuller, H. Best bang for your buck: GPU nodes for GROMACS biomolecular simulations. *J. Comput. Chem.* **2015**, *36*, 1990−2008.
(39) Irwin, J. J.; Shoichet, B. K. ZINC - A free database of commercially available compounds for virtual screening. *J. Chem. Inf. Model.* **2005**, *45*, 177−182.
(40) Tice, C. M. Selecting the right compounds for screening: Does Lipinski's rule of 5 for pharmaceuticals apply to agrochemicals? *Pest Manage. Sci.* **2001**, *2001*, 3−16.
(41) Schüttelkopf, A. W.; Van Aalten, D. M. F. PRODRG: A tool for high-throughput crystallography of protein-ligand complexes. *Acta Crystallogr. Sect. D Biol. Crystallogr.* **2004**, *60*, 1355−1363.
(42) George, D. C. P.; Chakraborty, C.; Haneef, S. S.; Nagasundaram, N.; Chen, L.; Zhu, H. Evolution- and Structure-Based Computational Strategy Reveals the Impact of Deleterious Missense Mutations on MODY 2 (Maturity-Onset Diabetes of the Young , Type 2). *Theranostics* **2014**, *4*, 366−385.
(43) Dvir, H.; Silman, I.; Harel, M.; Rosenberry, T. L.; Sussman, J. L. Acetylcholinesterase: From 3D Structure to Function. *Chem.-Biol. Interact.* **2010**, *187*, 10−22.
(44) Johnson, G.; Moore, S. The Peripheral Anionic Site of Acetylcholinesterase : Structure , Functions and Potential Role in Rational Drug Design. *Curr. Pharm. Des.* **2006**, *12*, 217−225.
(45) Friesner, R. A.; Murphy, R. B.; Repasky, M. P.; Frye, L. L.; Greenwood, J. R.; Halgren, T. A.; Sanschagrin, P. C.; Mainz, D. T. Extra precision glide: docking and scoring incorporating a model of hydrophobic enclosure for protein-ligand complexes. *J. Med. Chem.* **2006**, *49*, 6177−6196.
(46) Toutant, J.-P. Insect acetylcholinesterase: Catalytic properties, tissue distribution and molecular forms. *Prog. Neurobiol.* **1989**, *32*, 423−446.
(47) Toda, S.; Komazaki, S.; Tomita, T.; Kono, Y. Two amino acid substitutions in acetylcholinesterase associated with pirimicarb and organophosphorous insecticide resistance in the cotton aphid , *Aphis gossypii* Glover (Homoptera : Aphididae). *Insect Mol. Biol.* **2004**, *13*, 549−553.
(48) Zhen, C.; Miao, L.; Liang, P.; Gao, X. Survey of organophosphate resistance and an Ala216Ser substitution of acetylcholinesterase-1 gene associated with chlorpyrifos resistance in *Apolygus lucorum* (Meyer-Dür) collected from the transgenic Bt cotton fi elds in China. *Pestic. Biochem. Physiol.* **2016**, *132*, 29−37.

https://doi.org/10.1021/acsomega.1c07359
ACS Omega 2022, 7, 20515−20527

(49) Alon, M.; Alon, F.; Nauen, R.; Morin, S. Organophosphates' resistance in the B-biotype of *Bemisia tabaci* (Hemiptera : Aleyrodidae) is associated with a point mutation in an ace1 -type acetylcholinesterase and overexpression of carboxylesterase. *Insect Biochem. Mol. Biol.* **2008**, *38*, 940−949.

https://doi.org/10.1021/acsomega.1c07359
ACS Omega 2022, 7, 20515−20527